

Supplementary Materials for

Elucidating cellular population dynamics by molecular density function perturbations

Thanneer Malai Perumal ¹ and Rudiyanto Gunawan ^{2,3,*}

¹ Sage Bionetworks, Seattle, Washington, USA; thanneer.perumal@sagebase.org
² Institute for Chemical and Bioengineering, ETH Zurich, Zurich, Switzerland; rudi.gunawan@chem.ethz.ch
³ Swiss Institute of Bioinformatics, Lausanne, Switzerland
* Correspondence: rudi.gunawan@chem.ethz.ch; Tel.: +41-44-633-2134

Supplementary Material S1. Probability Distance Metrics

Signed Engineering Metric:

$$\Delta_E(f_{X_i}^A(t, x_i) \| f_{X_i}^B(t, x_i)) = \text{sign}(\Delta\mu_{X_i}) \int_{-\infty}^{\infty} (x_i f_{X_i}^A(t, x_i) - x_i f_{X_i}^B(t, x_i))^2 dx_i \quad (\text{S. 1})$$

Signed Jeffrey Divergence:

$$\Delta_{JD}(f_{X_i}^A(t, x_i) \| f_{X_i}^B(t, x_i)) = \text{sgn}(\Delta\mu_{X_i}) \int_{-\infty}^{\infty} (f_{X_i}^A(t, x_i) - f_{X_i}^B(t, x_i)) \ln \left(\frac{f_{X_i}^A(t, x_i)}{f_{X_i}^B(t, x_i)} \right) dx_i \quad (\text{S. 2})$$

Signed Kullback-Leibler Distance:

$$\Delta_{KLD}(f_{X_i}^A(t, x_i) \| f_{X_i}^B(t, x_i)) = \text{sgn}(\Delta\mu_{X_i}) \int_{-\infty}^{\infty} f_{X_i}^B(t, x_i) \ln \left(\frac{f_{X_i}^B(t, x_i)}{f_{X_i}^A(t, x_i)} \right) dx_i \quad (\text{S. 3})$$

Signed Jensen-Shannon Divergence:

$$\Delta_{JSD}(f_{X_i}(t, x_i)) = \text{sgn}(\Delta\mu_{X_i}) \frac{f_{X_i}^+(t, x_i) + f_{X_i}^-(t, x_i)}{2} \quad (\text{S. 4})$$

Signed Kolmogorov-Smirnov Metric:

$$\Delta_{KS}(f_{X_i}^A(t, x_i) \| f_{X_i}^B(t, x_i)) = \text{sgn}(\Delta\mu_{X_i}) \sup |F_{X_i}^A(t, x_i) - F_{X_i}^B(t, x_i)| \quad (\text{S. 5})$$

Supplementary Material S2. TRAIL induced programmed cell death model of Hela cells [1, 2]

State Variable	Definition
L	Death ligand, such as TRAIL and TNF
R	Inactive receptor complex
Rs	Active receptor complex
flip	FLICE inhibitory proteins inhibiting active receptors
C8	Procaspsase 8 and 10, inactive form of caspase 8 and 10
C8s	Cleaved caspase 8 and 10, active form of caspase 8 and 10
Bar	Bifunctional apoptosis regulator, binds to active caspase 8 and 10 acting as an inhibitor
C3	Procaspsase 3 and 7, inactive form of caspase 3 and 7
C3s	Cleaved caspase 3 and 7, active form of caspase 3 and 7
C6	Procaspsase 6, inactive form of caspase 6
C6s	Cleaved caspase 6, active form of caspase 6
XIAP	X-linked inhibitor of apoptosis protein
PARP	Poly ADP ribose polymerase, a DNA damage repair enzyme representing all substrates of cleaved caspase 3
cPARP	Cleaved poly ADP ribose polymerase measuring single cell death

Bid	BH3 interacting domain, substrate of cleaved caspase 8, inactive form
tBid	Truncated BH3 interacting domain, active form of Bid
Bcl2c	Cleaved B-cell lymphoma 2 represents the family of apoptotic proteins in the cellular compartment (CC), it binds to tBid and acts as inhibitor
Bax	Bcl2 associated X protein, substrate of tBid, inactive form
Baxs	Substrate of Bcl2 associated X protein, active form
Baxms	Active Baxs in mitochondrial compartment
Bcl2	All antiapoptotic proteins in the mitochondrial compartment
Bax2	Complex of Baxms and Baxms in mitochondria
Bax4	Complex of Bax2 and Bax2
M	Number of unoccupied Bax4 binding sites on outer membrane of the mitochondria in mitochondrial compartment
Ms	Number of pores Bax4 created on the outer membrane of the mitochondria
CyCm	Cytochrome C inside the mitochondria
CyCr	Cytochrome C released from the mitochondria, but remaining in the mitochondrial membrane
Smacm	Smac/Diablo homolog inside mitochondria

Smacr	Smac/Diablo released from the mitochondria, but remaining in the mitochondrial membrane
CyCc	Cytochrome C in the cellular compartment
Apaf	Apoptosis activating factor (Apaf-1), substrate of cytochrome C, inactive form
Apafs	Active form of Apaf-1
C9	Procaspase 9, inactive form
Apop	Apafs-C9 complex apoptosome
Smacc	Smac/Diablo in the cellular compartment
C3s:Ub	Caspase 3 ubiquitinated and targeted for degradation, inactive form
Pseudo:Variable	Pseudo variable with random initial condition and zero dynamics

Rate Equations:

r1 = kf1*L*R - kr1*L:R
r2 = kf2*L:R
r3 = kf3*C8*Rs - kr3*Rs:C8
r4 = kf4*Rs:C8
r5 = kf5*C3*C8s - kr5*C8s:C3
r6 = kf6*C8s:C3
r7 = kf7*C3s:PARP - kr7*C3s:PARP
r8 = kf8*C3s:PARP
r9 = kf9*Bid*C8s - kr9*C8s:Bid
r10 = kf10*C8s:Bid
r11 = kf11*Bax*tBid - kr11*tBid:Bax
r12 = kf12*tBid:Bax
r13 = kf13*Baxs - kr13*Baxms
r14 = (kf14*(Baxms*Baxms))/v - kr14*Bax2
r15 = (kf15*(Bax2*Bax2))/v - kr15*Bax4
r16 = (kf16*Bax4*M)/v - kr16*Bax4:M
r17 = kf17*Bax4:M
r18 = (kf18*CyCm*Ms)/v - kr18*Ms:CyCm
r19 = kf19*Ms:CyCm
r20 = kf20*CyCr - kr20*CyCc
r21 = (kf21*Ms*Smacm)/v - kr21*Ms:Smacm
r22 = kf22*Ms:Smacm
r23 = kf23*Smacr - kr23*Smacc
r24 = kf24*Apaf*CyCc - kr24*CyCc:Apaf
r25 = kf25*CyCc:Apaf
r26 = kf26*Apafs*C9 - kr26*Apop
r27 = kf27*Apop*C3 - kr27*Apop:C3
r28 = kf28*Apop:C3

r29 = kf29*C3s*C6 - kr29*C3s:C6
r30 = kf30*C3s:C6
r31 = kf31*C6s*C8 - kr31*C6s:C8
r32 = kf32*C6s:C8
r33 = kf33*Rs*flip - kr33*Rs:flip
r34 = kf34*Bar*C8s - kr34*C8s:Bar
r35 = kf35*Bcl2c*tBid - kr35*tBid:Bcl2c
r36 = (kf36*Baxms*Bcl2)/v - kr36*Baxms:Bcl2
r37 = (kf37*Bax2*Bcl2)/v - kr37*Bax2:Bcl2
r38 = (kf38*Bax4*Bcl2)/v - kr38*Bax4:Bcl2
r39 = kf39*Smacc*XIAP - kr39*Smacc:XIAP
r40 = kf40*Apop*XIAP - kr40*Apop:XIAP
r41 = kf41*C3s*XIAP - kr41*C3s:XIAP
r42 = kf42*C3s:XIAP

Ordinary differential equations

d[L]/dt = -r1
d[R]/dt = -r1
d[L:R]/dt = r1 -r2
d[Rs]/dt = r2 -r3 +r4 -r33
d[flip]/dt = -r33
d[Rs:flip]/dt = r33
d[C8]/dt = -r3 -r31
d[Rs:C8]/dt = r3 -r4
d[C8s]/dt = r4 -r5 +r6 -r9 +r10 +r32 -r34
d[Bar]/dt = -r34
d[C8s:Bar]/dt = r34
d[C3]/dt = -r5 -r27
d[C8s:C3]/dt = r5 -r6
d[C3s]/dt = r6 -r7 +r8 +r28 -r29 +r30 -r41
d[C6]/dt = -r29
d[C3s:C6]/dt = r29 -r30
d[C6s]/dt = r30 -r31 +r32
d[C6s:C8]/dt = r31 -r32
d[XIAP]/dt = -r39 -r40 -r41 +r42
d[C3s:XIAP]/dt = r41 -r42
d[PARP]/dt = -r7
d[C3s:PARP]/dt = r7 -r8
d[cPARP]/dt = r8
d[Bid]/dt = -r9
d[C8s:Bid]/dt = r9 -r10
d[tBid]/dt = r10 -r11 +r12 -r35
d[Bcl2c]/dt = -r35
d[tBid:Bcl2c]/dt = r35

d[Bax]/dt = -r11
d[tBid:Bax]/dt = r11 -r12
d[Baxs]/dt = r12 -r13
d[Baxms]/dt = r13 -2*r14 -r36
d[Bcl2]/dt = -r36 -r37 -r38
d[Baxms:Bcl2]/dt = r36
d[Bax2]/dt = r14 -2*r15 -r37
d[Bax2:Bcl2]/dt = r37
d[Bax4]/dt = r15 -r16 -r38
d[Bax4:Bcl2]/dt = r38
d[M]/dt = -r16
d[Bax4:M]/dt = r16 -r17
d[Ms]/dt = r17 -r18 +r19 -r21 +r22
d[CyCm]/dt = -r18
d[Ms:CyCm]/dt = r18 -r19
d[CyCr]/dt = r19 -r20
d[Smacm]/dt = -r21
d[Ms:Smacm]/dt = r21 -r22
d[Smacr]/dt = r22 -r23
d[CyCc]/dt = r20 -r24 +r25
d[Apaf]/dt = -r24
d[CyCc:Apaf]/dt = r24 -r25
d[Apafs]/dt = r25 -r26
d[C9]/dt = -r26
d[Apop]/dt = r26 -r27 +r28 -r40
d[Apop:C3]/dt = r27 -r28
d[Smacc]/dt = r23 -r39
d[Apop:XIAP]/dt = r40
d[Smacc:XIAP]/dt = r39
d[C3s:Ub]/dt = r42
d[Pseudo:Variable]/dt = 0

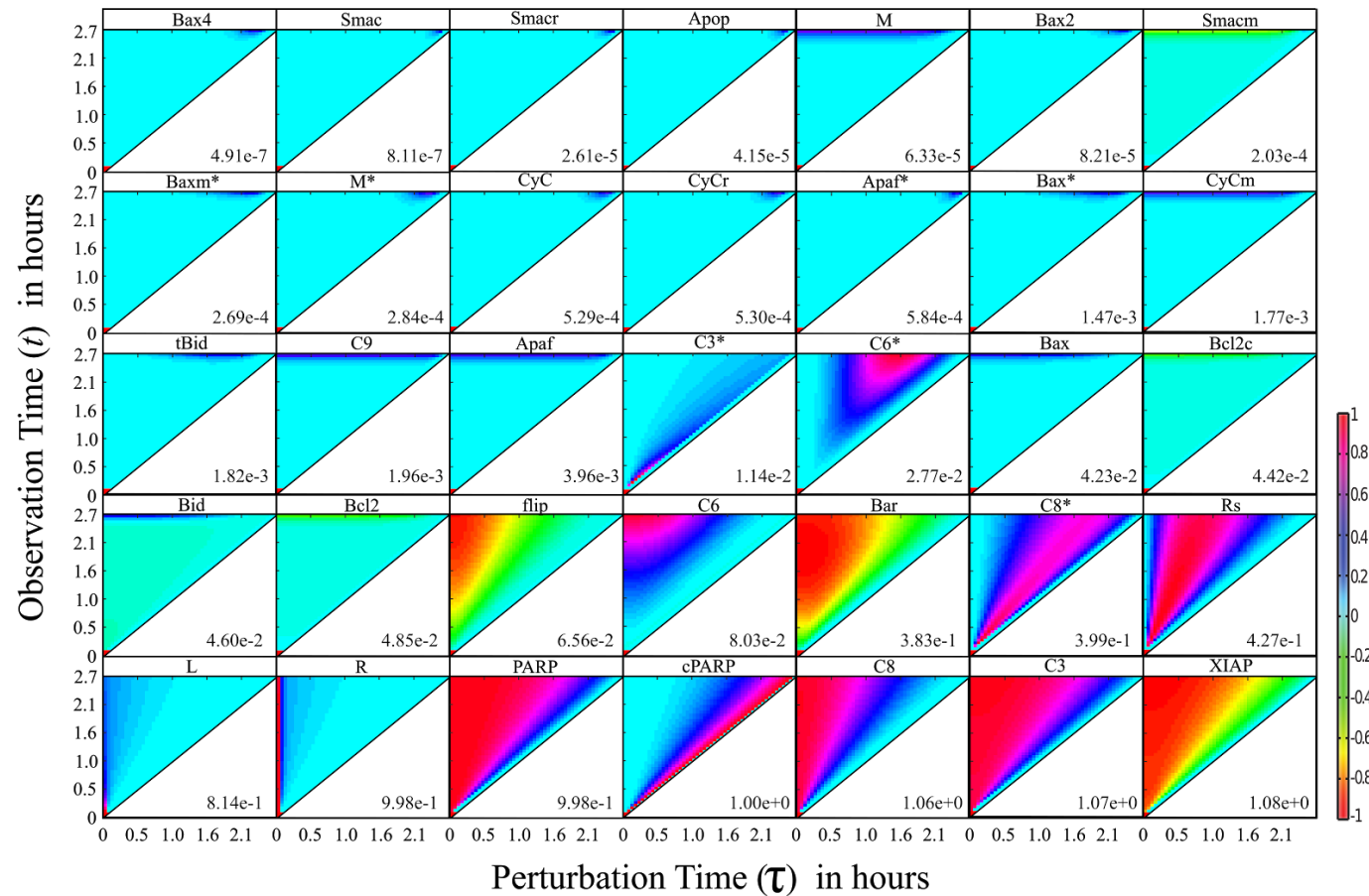
Initial Conditions:	#/cell	Coefficient of variation
L	15000	0
R	200	0.25
L:R	0	0
Rs	0	0
flip	100	0.25
Rs:flip	0	0
C8	20000	0.25
Rs:C8	0	0
C8s	0	0
Bar	1000	0.25
C8s:Bar	0	0
C3	10000	0.282
C8s:C3	0	0
C3s	0	0
C6	10000	0.25
C3s:C6	0	0
C6s	0	0
C6s:C8	0	0
XIAP	100000	0.288
C3s:XIAP	0	0
PARP	1000000	0.25
C3s:PARP	0	0
cPARP	0	0
Bid	40000	0.288
C8s:Bid	0	0
tBid	0	0
Bcl2c	20000	0.25
Bid:Bcl2c	0	0
Bax	100000	0.271

tBid:Bax	0	0
Baxs	0	0
Baxms	0	0
Bcl2	20000	0.294
Baxms:Bcl2	0	0
Bax2	0	0
Bax2:Bcl2	0	0
Bax4	0	0
Bax4:Bcl2	0	0
M	500000	0.25
Bax4:M	0	0
Ms	0	0
CyCm	500000	0.25
Ms:CyCm	0	0
CyCr	0	0
Smacm	100000	0.25
Ms:Smacm	0	0
Smacr	0	0
CyC	0	0
Apaf	100000	0.25
CyC:Apaf	0	0
Apafs	0	0
C9	100000	0.25
Apop	0	0
Apop:C3	0	0
Smac	0	0
Apop:XIAP	0	0
Smac:XIAP	0	0
C3s:Ub	0	0
Pseudo	1	0

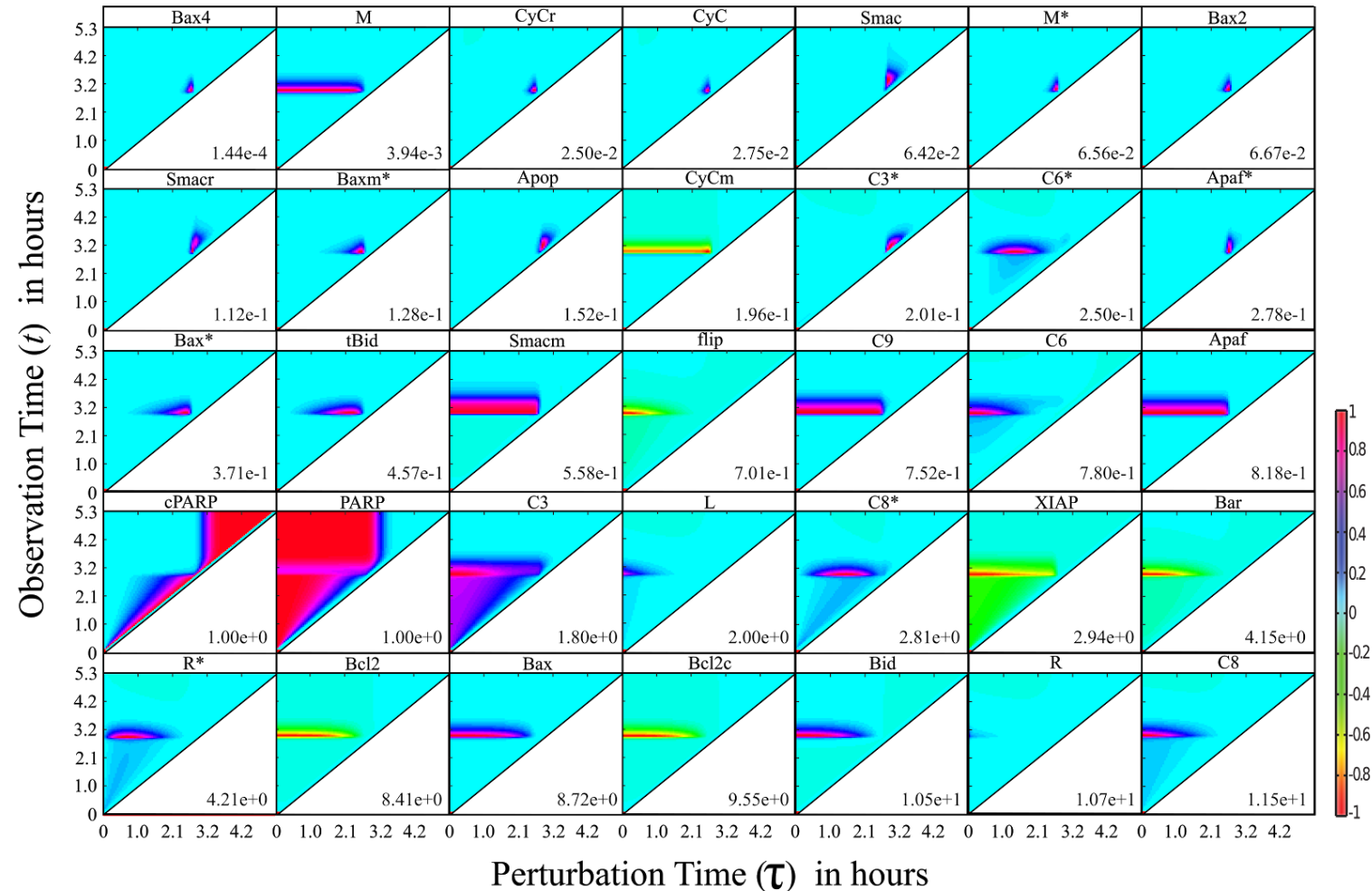
Rate Constants:	(#/CC)⁻¹.sec⁻¹	Rate Constants:	sec⁻¹	Rate Constants:	sec⁻¹
Kf1	4.00E-07	kr1	1.00E-03	kf2	1.00E-05
Kf3	1.00E-06	kr3	1.00E-03	kf4	1.00E+00
Kf5	1.00E-07	kr5	1.00E-03	kf6	1.00E+00
Kf7	1.00E-06	kr7	1.00E-02	kf8	1.00E+00
Kf9	1.00E-07	kr9	1.00E-03	kf10	1.00E+00
Kf11	1.00E-07	kr11	1.00E-03	kf12	1.00E+00
Kf13	1.00E-02	kr13	1.00E-02	kf17	1.00E+00
Kf14	1.00E-06	kr14	1.00E-03	kf19	1.00E+01
Kf15	1.00E-06	kr15	1.00E-03	kf22	1.00E+01
Kf16	1.00E-06	kr16	1.00E-03	kf25	1.00E+00
Kf18	2.00E-06	kr18	1.00E-03	kf28	1.00E+00
Kf20	1.00E-02	kr20	1.00E-02	kf30	1.00E+00
Kf21	2.00E-06	kr21	1.00E-03	kf32	1.00E+00
Kf23	1.00E-02	kr23	1.00E-02	kf42	1.00E-01
Kf24	5.00E-07	kr24	1.00E-03		
Kf26	5.00E-08	kr26	1.00E-03		
Kf27	5.00E-09	kr27	1.00E-03		
Kf29	1.00E-06	kr29	1.00E-03		
Kf31	3.00E-08	kr31	1.00E-03		
Kf33	1.00E-06	kr33	1.00E-03		
Kf34	1.00E-06	kr34	1.00E-03		
Kf35	1.00E-06	kr35	1.00E-03		
Kf36	1.00E-06	kr36	1.00E-03		
Kf37	1.00E-06	kr37	1.00E-03		
Kf38	1.00E-06	kr38	1.00E-03		
Kf39	7.00E-06	kr39	1.00E-03		
Kf40	2.00E-06	kr40	1.00E-03		
Kf41	2.00E-06	kr41	1.00E-03		

Ratio of mitochondrial volume to cell volume (v) is taken as 0.07

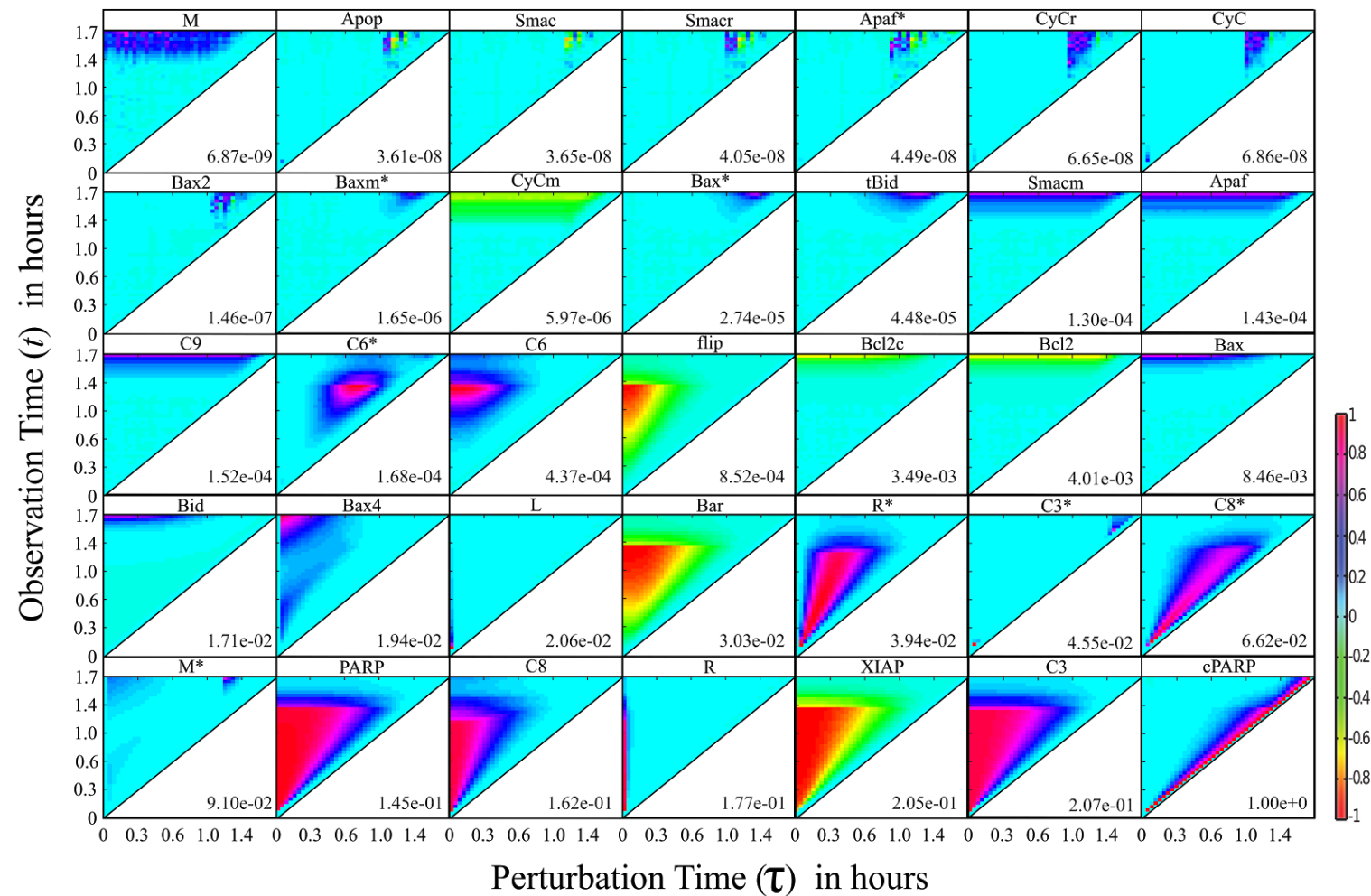
Supplementary Figures



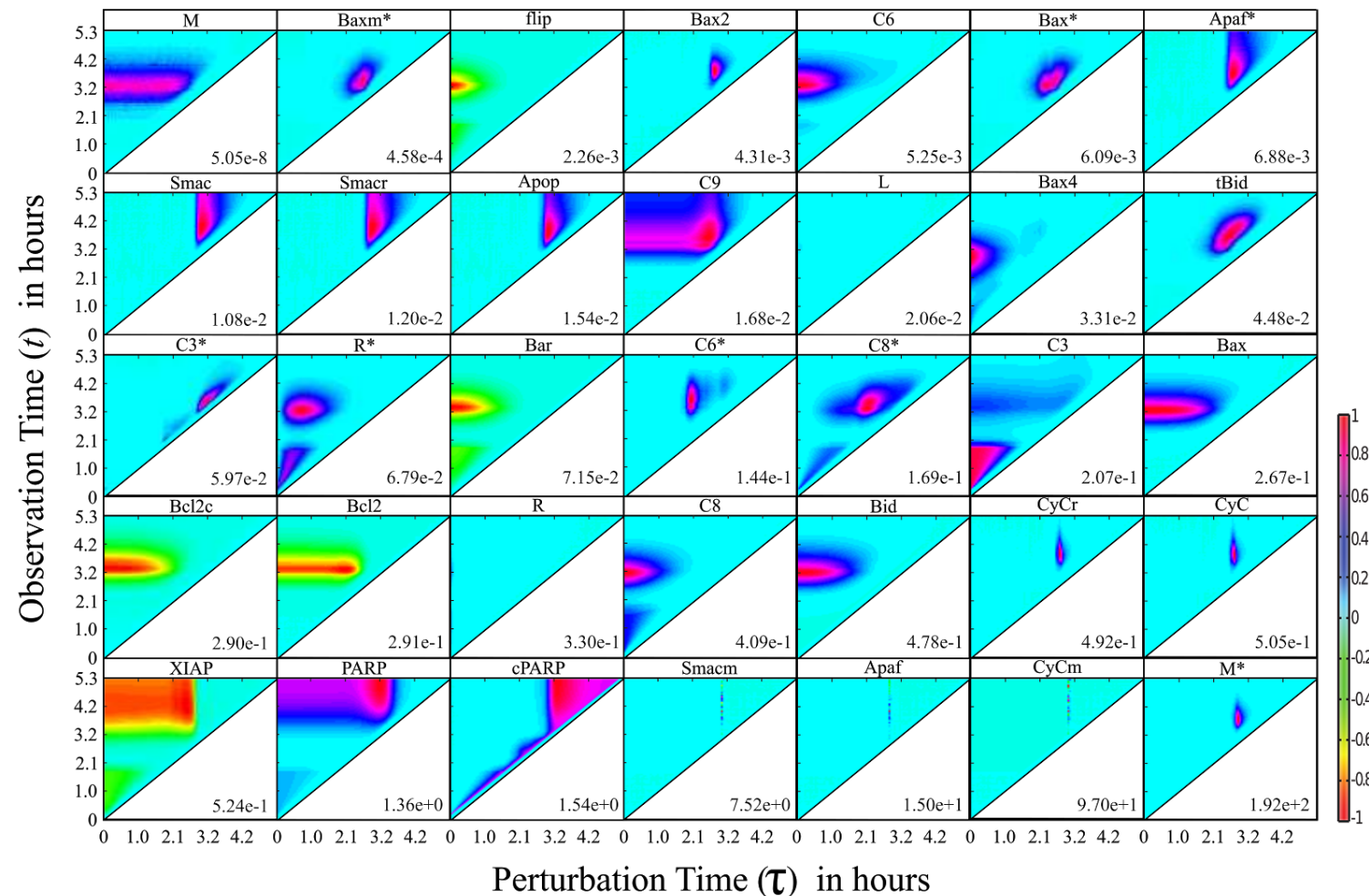
Supplementary Figure S1. GFM analysis of TRAIL induced apoptosis model during pre-MOMP (before 2.36 hours). The subplots give the heat maps of the GFM coefficients of cPARP levels with respect to an infinitesimal perturbations to each of the molecules. The heat maps are arranged in increasing magnitude of peak sensitivities (i.e. scaling factor shown in the bottom right corner).



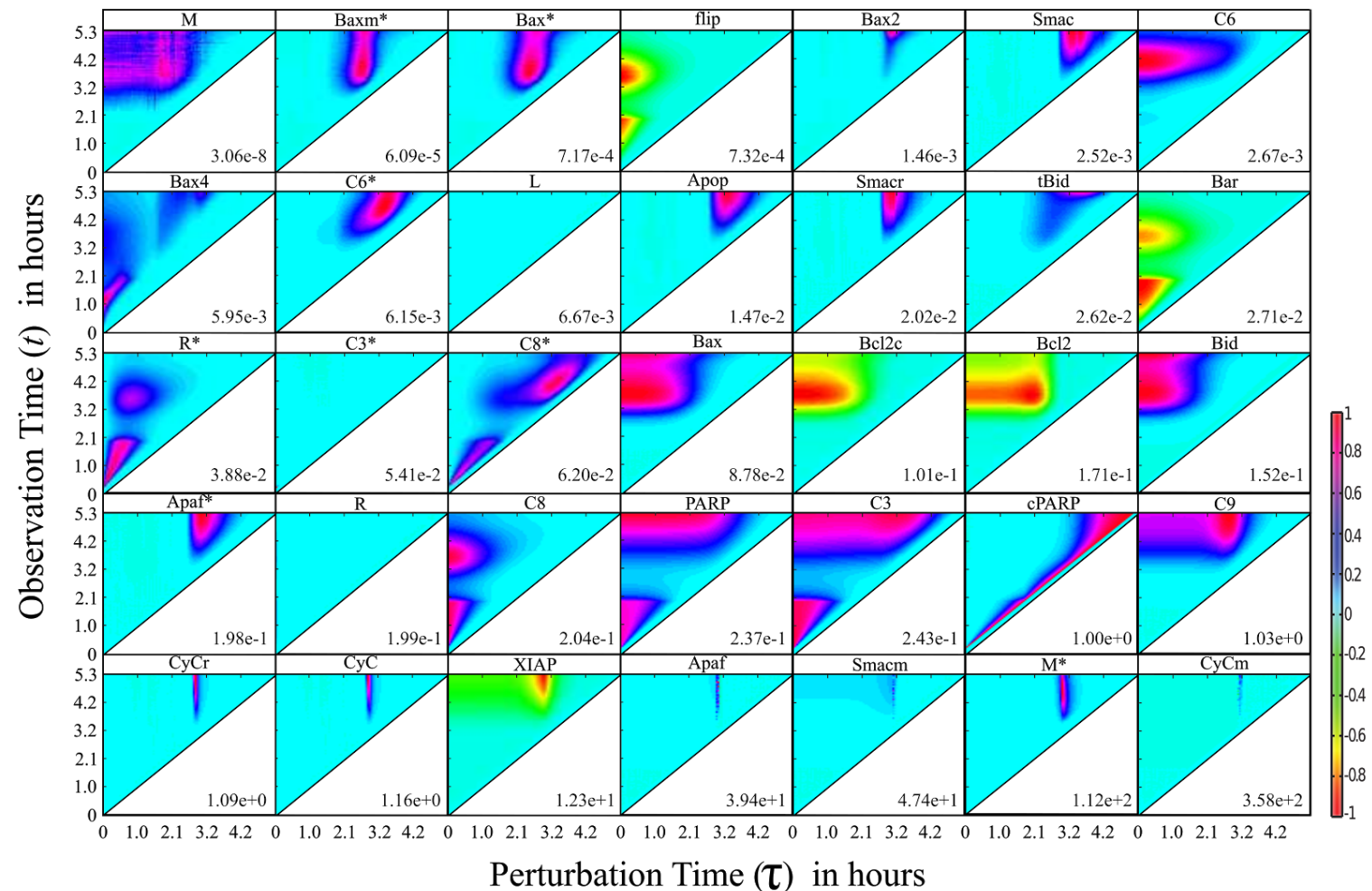
Supplementary Figure S2. GFM analysis of TRAIL induced apoptosis model during post-MOMP (after 2.36 hours). The subplots give the heat maps of the GFM coefficients of cPARP levels with respect to an infinitesimal perturbations to each of the molecules. The heat maps are arranged in increasing magnitude of peak sensitivities (i.e. scaling factor shown in the bottom right corner).



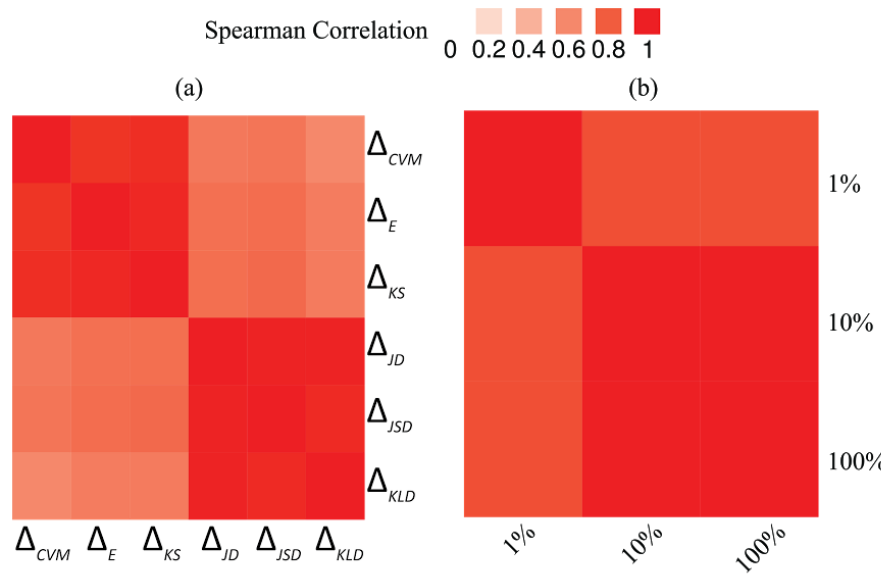
Supplementary Figure S3. MDFP analysis of TRAIL induced apoptosis model during pre-MOMP (before 1.76 hours). The subplots give the heat maps of the MDFP coefficients of cPARP levels with respect to a mean-shift perturbations to each of the molecules. The heat maps are arranged in increasing magnitude of peak sensitivities (i.e. scaling factor shown in the bottom right corner).



Supplementary Figure S4. MDFP analysis of TRAIL induced apoptosis model during post-MOMP (after 1.76 hours). The subplots give the heat maps of the MDFP coefficients of cPARP levels with respect to a mean-shift perturbations to each of the molecules. The heat maps are arranged in increasing magnitude of peak sensitivities (i.e. scaling factor shown in the bottom right corner).



Supplementary Figure S5: MDFP analysis of non-apoptotic Hela subpopulation. The subplots give the heat maps of the MDFP coefficients of cPARP levels with respect to a mean-shift perturbations to each of the molecules. The heat maps are arranged in increasing magnitude of peak sensitivities (i.e. scaling factor shown in the bottom right corner).



Supplementary Figure S6: Spearman correlations of MDFFP sensitivity coefficients using different distribution distances and perturbation sizes. (a) Correlation of the MDFFP sensitivity coefficients calculated using different distribution distances with a 10% mean perturbation. (b) Correlation of the MDFFP sensitivity coefficients calculated using different sizes (1%, 10% and 100%) of mean perturbations with the Cramer-von Mise distance (Δ_{CVM}).

References

1. Spencer, S. L.; Gaudet, S.; Albeck, J. G.; Burke, J. M.; Sorger, P. K. Non-genetic origins of cell-to-cell variability in TRAIL-induced apoptosis. *Nature* **2009**, *459*, 428–432.
2. Albeck, J. G.; Burke, J. M.; Spencer, S. L.; Lauffenburger, D. A.; Sorger, P. K. Modeling a snap-action, variable-delay switch controlling extrinsic cell death. *PLoS Biol.* **2008**, *6*, 2831–2852.